JOURNAL OF MATERIALS SCIENCE 28 (1993) 3409–3422

Interface characterization by TEM, AES and SIMS in tough SiC (ex-PCS) fibre-SiC (CVI) matrix composites with a BN interphase

O. DUGNE, S. PROUHET, A. GUETTE, R. NASLAIN
Laboratoire des Composites Thermostructuraux (UMR 47 CNRS-SEP-UB1), Domaine Universitaire, 3 Allée de la Boëtie, F-33600-Pessac, France

R. FOURMEAUX, Y. KHIN, J. SEVELY
Laboratoire d'Optique Electronique-CEMES (CNRS), 29 rue Jeanne Marvig, F-31055-Toulouse, France

J. P. ROCHER and J. COTTERET
Société Européenne de Propulsion, B.P. 37, F-33165-Saint-Médard-en-Jalles, France

The fibre–matrix interfacial zone formed during the isothermal/isobaric chemical vapour infiltration processing of SiC fibres (ex-polycarbosilane)/boron nitride/SiC matrix composites has been analysed by TEM/electron energy loss spectroscopy, Auger electron spectroscopy, and secondary ion mass spectroscopy. In the composites, the boron nitride interphase (deposited from BF_3–NH_3) is made of turbostratic boron nitride, almost stoichiometric but containing some oxygen (less than 5 at %). The boron nitride layer stacks are randomly orientated except in the very vicinity of the fibre surface where they lie almost parallel to the substrate. The long chemical vapour infiltration treatment at 1000 °C used to infiltrate the SiC matrix acts as an annealing treatment for the metastable ex-polycarbosilane fibres which gives rise to the growth of an SiO_2/carbon amorphous double layer at the boron nitride/fibre interface. Deflection of microcracks arising from the failure of the brittle SiC-matrix occurs at the boron nitride/SiO_2 interface considered to be the weaker link in the matrix/boron nitride interphase/SiO_2/carbon/fibre sequence. It is suggested that the combination of the boron nitride layered interphase and SiO_2/carbon fibre decomposition products might play an important role in determining the propagation path of microcracks in the fibre/matrix interfacial zones and could be responsible, at least to some extent, for the non-brittle behaviour of such composites.

1. Introduction

Ceramic matrix composites (CMCs) made from SiC (ex-polycarbosilane or PCS) fibres (the most commonly used being the Nicalon fibres, Nippon Carbon) usually exhibit a brittle mechanical behaviour unless the fibre–matrix coupling has been properly optimized during the high-temperature step of their processing. It is now well accepted that tough CMCs are obtained when a thin layer of a soft material, referred to as the interphase, is formed at the fibre–matrix interfaces as the result of: (i) some chemical reaction taking place *in situ* at high temperature during processing (related to, for example, a thermal decomposition of the fibre material or an interdiffusion between the fibre and the matrix), or (ii) a treatment of the surface of the fibres (e.g. a chemical vapour deposition (CVD) coating) prior to embedding in the matrix. The main role played by the interphase is to act as a mechanical fuse in order to protect the brittle fibres against the notch effect arising from the microcracking of the matrix (in a CMC submitted to an increasing load, the matrix fails first). Microcracks propagating in the brittle matrix usually in Mode I are either arrested or even deflected in Mode II (with, in the latter case, a debonding of the fibres) with the result that: (i) the fibres which are not broken when the matrix fails can be further loaded up to their intrinsic failure stress and (ii) the composite exhibits a tough mechanical behaviour [1–3]. Apart from its role of mechanical fuse, the interphase, particularly when it is deposited by CVD, may also act as a diffusion barrier to protect the fibres against chemical reactions involving the matrix or the gaseous atmosphere.

Among the few soft materials which have been selected as interphases in SiC, ZrO_2, mullite or glass–ceramic matrix composites, pyrocarbon and boron nitride (BN), both having a turbostratic layered crystal structure, are those which have resulted so far in the best mechanical properties, particularly in terms of toughness [4–14]. Furthermore from a chemical

0022–2461

standpoint, the oxidation of BN is known to start at a higher temperature than that of pyrocarbon. It also yields an oxide, i.e. B_2O_3, which remains in a condensed state (and thus may play a protection role) over a rather wide temperature range, whereas the oxidation of pyrocarbon gives only gaseous oxides. Therefore, a BN interphase could be a better interphase material for composites used in oxidizing atmospheres and medium temperatures.

It has already been shown that a BN interphase can be deposited either by CVD on filaments or tows as well as by chemical vapour infiltration (CVI) in fibrous preforms, from a variety of precursors including (i) B_2H_6–NH_3 or BX_3–NH_3 (with X = F,Cl) mixtures [15–20] or (ii) organometallic species such as polyborazine or aminoborane and hexachloroborazene [21–23]. However, and as far as we know, no detailed investigation of the actual composition, structure and microstructure of the BN interphase in CMCs has yet been published.

The aim of the present contribution is to report the data that we have obtained, from TEM, Auger electron spectroscopy (AES) and secondary ion mass spectroscopy (SIMS) analyses performed on SiC (ex-PCS)/BN/SiC (CVI) composites, on a turbostratic BN interphase infiltrated in fibre preforms from a BF_3–NH_3 precursor. Another objective of the present work was to study the change that occurs during the processing of the composites either in the BN interphase itself or at both the interphase/fibre and interphase/matrix interfaces.

2. Experimental procedure

2.1. Materials

The material used in the present investigation is a composite prepared according to a two-step CVI procedure, from a two-dimensional preform (90 mm × 90 mm × 10 mm) made of continuous SiC (ex-PCS) fibres (Nicalon (NLP 201 grade) fibre, Nippon Carbon). The preform consisted of a stack of fabrics maintained together with a ceramic tooling and whose initial porosity was of the order of 37%.

In the first CVI step, the BN-interphase material was deposited within the preform porosity, from a BF_3–NH_3 mixture (with a molar NH_3/BF_3 ratio slightly higher than unity) at a temperature of about 1000 °C and under reduced pressure, according to a procedure which has been described elsewhere [16, 17]. The thickness of the interphase layer was of the order of 1 μm which corresponded to an infiltration duration of about 20 h. At this step, the consolidated preform will be referred to as 2D-SiC/BN preform, although it is now well established that such fibres (i) are not pure SiC but rather a nanometrescale mixture of SiC + C in an amorphous Si-(C,O) continuum, and (ii) have a surface which might be enriched in oxygen [24].

In the second CVI-step, the SiC matrix (consisting mainly of the β-SiC blende-type modification) was deposited within the porosity of the 2D-SiC/BN preform, from a CH_3SiCl_3/H_2 precursor, also at about 1000 °C and under reduced pressure, according to the isothermal/isobaric CVI process (ICVI) which has been presented elsewhere [25, 26]. In order to achieve a residual porosity of about $V_p = 10\%–15\%$, an overall infiltration time of several hundreds of hours was necessary, a well-known feature of the ICVI process [27]. At this step, the material will be referred to as 2D-SiC/BN/SiC composite.

It is worthy of note that the various analyses mentioned in the following have been performed on the same material plate at each processing step. SiC (ex-PCS) fibres coated with the BN interphase were extracted from fragments of tows protruding from the external surface of the plate, after the first CVI step. In the same manner, the sample used to characterize the BN interphase, after the second CVI step, was cut by diamond-saw cutting from the outside of the 2D-SiC/BN/SiC composite plate, whose central part was kept for mechanical testing [28].

Furthermore, in order to assess the possible effect of the thermal treatments corresponding to the CVI steps, on the ex-PCS SiC fibres (which are known to be in a non-equilibrium state after processing), two additional experiments were performed on the as-received fibres: (i) a heating/cooling cycle from room temperature to 1000 °C under vacuum in the BN/CVI furnace, which simulated the transient thermal/chemical regime seen by the 2D-SiC preform prior to the BF_3–NH_3 stream was allowed to flow in the infiltration chamber (heat treatment 1) and (ii) a long duration annealing at 1000 °C (i.e. about 800 h under vacuum thought to simulate that seen by the fibres during the SiC CVI step (which is usually shorter) (heat treatment 2).

2.2. Analysis

2.2.1. Auger electron spectroscopy (AES)

AES analyses were performed with a scanning microanalyser (PHI 560 SAM, Physical Electronics/Perkin Elmer) under the following conditions: a lateral resolution of about 1 μm, a residual pressure of 10^{-7} Pa, a high voltage of 5 kV and an electron-beam current of 80 nA in the sample. The experiments were performed according to the depth profiling mode with a sputtering Ar^+ ion gun. The peak to peak heights of the derivative $d[(NE)]/dE$ spectra (B_{KLL}, N_{KLL}, O_{KLL}, C_{KLL} and Si_{LVV} transitions) were used to calculate semi-quantitatively atomic concentrations. The data will be presented as atomic concentration–sputtering time curves (no attempt was made to convert the sputtering time in sputtered depth owing to the complexity of the materials).

2.2.2. Secondary ion mass spectroscopy (SIMS)

SIMS analyses were performed with a microanalyser (SIMS Lab (MIG 300), Vacuum Generators) equipped with a liquid metal ion source (i.e. Ga^+). The lateral resolution was of about 50 nm and the residual pressure in the analysis chamber was maintained below 10^{-8} Pa. Owing to the insulating electrical character

of both the ex-PCS fibres [29] and BN interphases, the charge effect arising at the sample surface was compensated (at least partly) with an electron flood gun.

The analyses (performed by Science et Surfaces) were conducted according to the depth profile mode with a sputtering ion gun, the intensities of the secondary ion beams being recorded versus the sputtering time. The ions which have been selected are: $^{11}B^+$, $^{28}Si^+$, $^{16}O^-$, $^{19}F^-$, $^{24}C_2^-$ and $^{26}C_2H_2^-/^{26}CN^-$. In fact, all the analyses which have been performed should be regarded as only qualitative. No attempt was made to derive atomic concentrations from the recorded intensities of the secondary ion beams owing to the occurrence of a strong matrix effect. As an example, the intensity of the $^{28}Si^+$ beam is strongly enhanced for silicon atoms in silica. Conversely, because nitrogen is known to be characterized by a low yield in secondary ions, it is common to select the $^{26}CN^-$ ion as a nitrogen vector which has the same mass as the $^{26}C_2H_2^-$ ion.

2.2.3. Transmission electron microscopy (TEM)

TEM analyses were performed with a 120 kV electron microscope (EM 400 T, Philips) equipped with an electron energy loss spectrometer (EELS) (ELS 50, Vacuum Generators). The apparatus was used, respectively, (i) to characterize the crystal structure and the texture of the materials by selected-area diffraction (SAD) patterns and bright-field images, and (ii) to determine the chemical composition of the materials at a submicroscopic scale by electron energy loss spectroscopy (EELS).

The thin foils were prepared according to two different procedures: those of individual filaments were obtained by ultramicrotomy, whereas those of the composites were prepared by mechanical thinning and ion milling (600, Gatan).

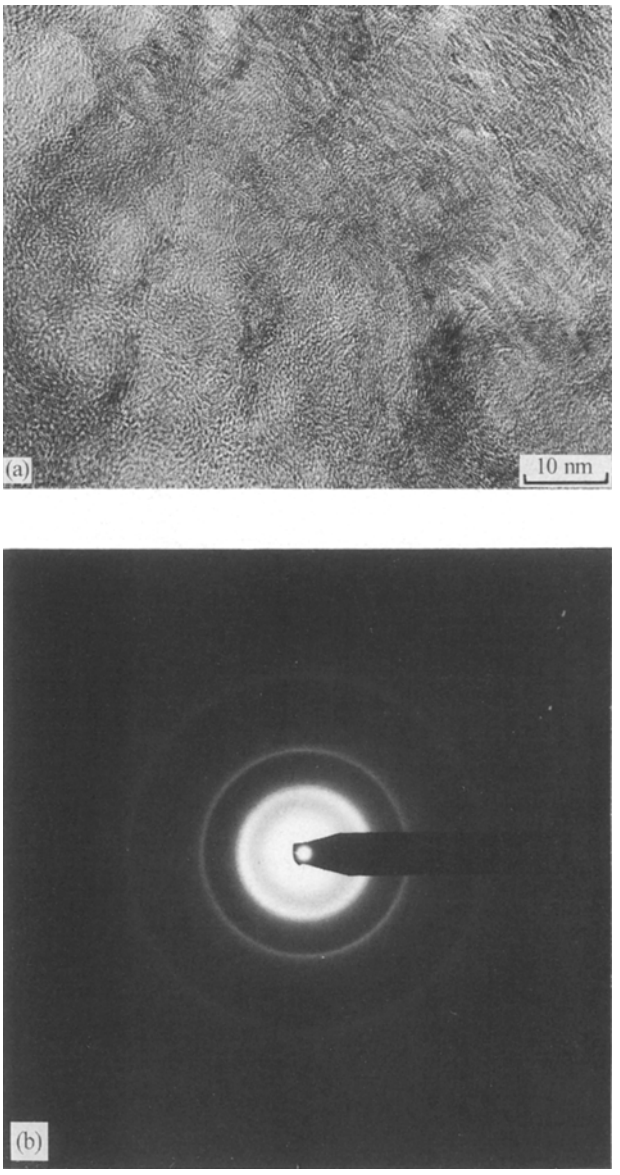

Figure 1 TEM analysis of a BN interphase as infiltrated in a SiC (ex-PCS) fibrous preform from a BF_3–NH_3 precursor: (a) bright field image, (b) SAD pattern.

3. Results

3.1. Characterization of the BN-coated SiC fibres after the first CVI step

3.1.1. The boron nitride fibre coating

The BN films deposited from a BF_3–NH_3 precursor under CVI conditions (i.e. at low temperature and pressure) either on flat SiC substrates or SiC (ex-PCS) fibres have been studied in detail elsewhere [30]. In the particular case considered here (i.e. that of 1 μm interphase deposited on SiC (ex-PCS) fibrous substrate, the TEM bright-field images and SAD data (Fig. 1) show that the BN deposits are turbostratic (absence of three-dimensional ordering of the hexagonal BN layers) with a rather large interlayer distance (d_{002} = 0.365 nm) with respect to that observed in hexagonal boron nitride deposited or annealed at very high temperatures (d_{002} = 0.333 nm). Moreover, the deposits are made of randomly orientated crystals and contain numerous micropores (Fig. 1a).

As shown in Table I, the N/B atomic ratio in the as-infiltrated BN interphase is much lower than that expected from stoichiometry, i.e. it ranges from 0.7–0.8 (from EELS data) with respect to 1 in stoichiometric BN. Furthermore, the BN interphase contains significant amounts of oxygen (i.e. 10–15 at %).

3.1.2. The BN/fibre interface

The BN interphase is only weakly bonded to the fibre surface as evinced from the occurrence of easy debonding at the interphase/fibre interface (Fig. 2). When debonded from the BN interphase, the fibre surface did not seem to have been extensively damaged chemically during the deposition of BN from BF_3–NH_3. However, microcavities were observed along the imprints left by the fibres in the boron nitride deposit (Fig. 2b).

From the various analyses which have been performed, it appears that both oxygen and carbon have piled up at the interface between the SiC (ex-PCS) fibre and the BN interphase (Figs 3 and 4). A detailed

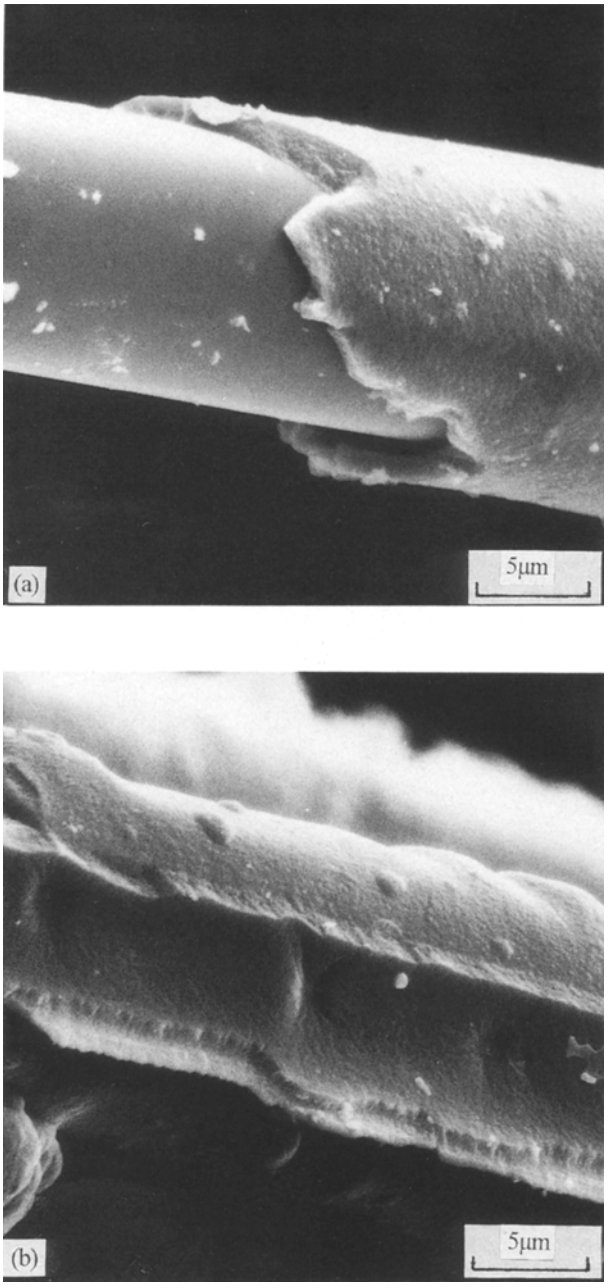

Figure 2 Fracture of a 2D-SiC/BN sample (after 20 h BN CVI) at the BN/SiC interface, as observed by scanning electron microscopy. (a) SiC (ex-PCS) fibre partly debonded from the BN deposit. (b) microscopic cavities in the imprint left by a SiC (ex-PCS) fibre in the BN deposit.

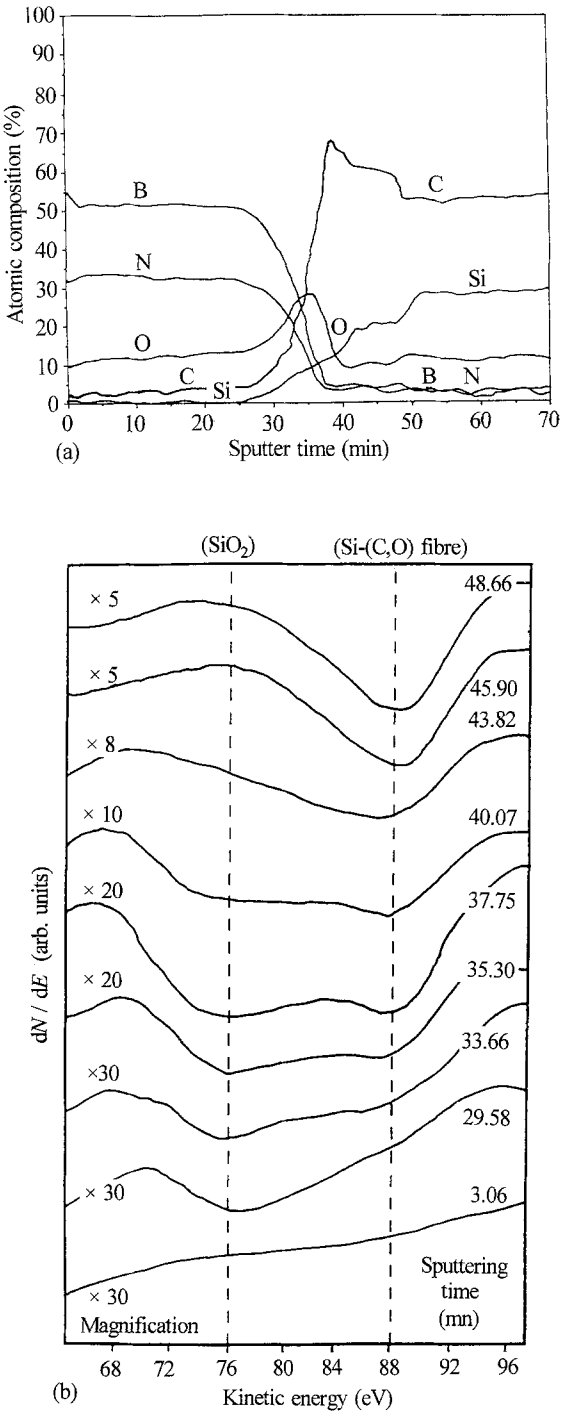

Figure 3 AES analysis of the BN interphase deposited by CVI (infiltration time 20 h) from a BF_3–NH_3 precursor, on an ex-PCS fibre: (a) depth–concentration profile along a direction perpendicular to the fibre surface, (b) high-resolution analysis of the Si_{LVV} transition recorded for increasing sputtering time.

analysis of the Si_{LVV} Auger electron transition recorded for different sputtering times along a direction perpendicular to the interface, suggests that the oxygen atoms which have piled up at that interface are bonded to silicon as in silica (Fig. 3b). For short sputtering times (the depth origin being in the BN interphases as shown in Fig. 3a), i.e. 30–40 min, the Auger electrons corresponding to the Si_{LVV} transition have the same kinetic energy to that observed in silica (76 eV) [31]. As sputtering proceeds, the Si_{LVV} peak at 76 eV progressively vanishes, whereas a new peak at 88 eV, close to that of the Si_{LVV} transition in SiC (92 eV) and assigned to the silicon atoms from the ex-PCS SiC fibres [32, 33] is observed with an increasing intensity. For still longer sputtering times, i.e. 40–50 min, the depth concentration profiles clearly support the occurence of another sublayer consisting mainly of carbon (Fig. 3a). However, no significant chemical shift or shape changes were observed for the Auger electron related to the C_{KLL} transition.

The SIMS depth profiles confirm qualitatively that oxygen atoms have piled up at the fibre/BN interface as is apparent from the occurrence of sharp peaks in the intensity–sputtering times curves shown in Fig. 4a for the $^{16}O^-$ ion (sputtering time 165 s) and Fig. 4b for the $^{28}Si^+$ ion (sputtering time 196 s). As already mentioned in Section 2.2.2, the intensity of the $^{28}Si^+$ peak is strongly enhanced in the interfacial silica sublayer as

evinced from the fact that it is much higher than the corresponding intensity recorded in the ex-PCS SiC fibre itself (for sputtering times longer than 270 s) where silicon is present with a higher concentration, i.e. 57 at % instead of 33 at % in silica but in different chemical bonds, i.e. SiC and Si–(C,O). Despite the fact that the nitrogen concentration is high in the BN deposit, the intensity of the $^{26}CN^-$ secondary ion beam remains very low for sputtering times less than 150 s (Fig. 4a) which is consistent with the fact that BN films deposited from BF_3–NH_3 mixtures on a non-reactive substrate do not contain carbon, as reported elsewhere [34]. On the contrary, beyond this value, the intensity of the $^{28}CN^-$ secondary ion beam increases sharply with a well-defined peak at 186 s. A similar increase in intensity is also observed for the same sputtering time for the $^{24}C_2^-$ ion beam. These results are qualitatively consistent with (i) the occurrence of a carbon-rich interfacial sublayer between the fibre and silica and (ii) the high carbon concentration in the ex-PCS SiC fibre (i.e. 30 at % present as both SiC and free carbon). These data suggest that the ions of mass 28 are probably mainly $C_2H_2^-$ ions rather than CN^- ions at least for sputtering times larger than 222 s. Surprisingly, the $^{16}O^-$ ion beam intensity recorded for BN deposits is much higher than observed for the ex-PCS SiC fibre, although the oxygen concentration is about the same in both materials (i.e. 10–15 at % for BN as shown in Table I, compared with 12 at % in the fibre). Therefore, the formation of $^{16}O^-$ ions could be much easier in a BN-matrix than it is in the Si–(C,O) amorphous continuum of the ex-PCS SiC fibre. Finally, the fluorine depth profile curve exhibits a very sharp peak immediately beyond the silica sublayer suggesting that this element (whose occurrence has to be related to the BF_3–NH_3 precursor used for the deposition of BN) might be located in the carbon interfacial sublayer. Because fluorine has not been detected either by AES or by EELS, it is thought that its concentration might be low (i.e. of the order of 1% or even less, based on the AES and EELS detection limits).

The occurence of a thin silica layer is also consistent with the EELS spectrum recorded from a thin foil at the BN/fibre interface. As shown in Fig. 5, the only elements identified are silicon (L_{23} ionization edge at 100 eV) and oxygen (K ionization edge at 534 eV).

3.2. Characterization of the BN interphase in 2D-SiC/BN/SiC composites

As is clearly apparent from the transmission electron micrograph shown in Fig. 6, the transition between the ex-PCS SiC fibre and the SiC CVI matrix is complex when observed at a submicrometre scale. It involves at least three different phases which have been identified, as discussed below, at the BN interphase, a thin irregular sublayer of silica and a sublayer of carbon.

3.2.1. The boron nitride interphase

The chemical composition and the d_{002} interlayer

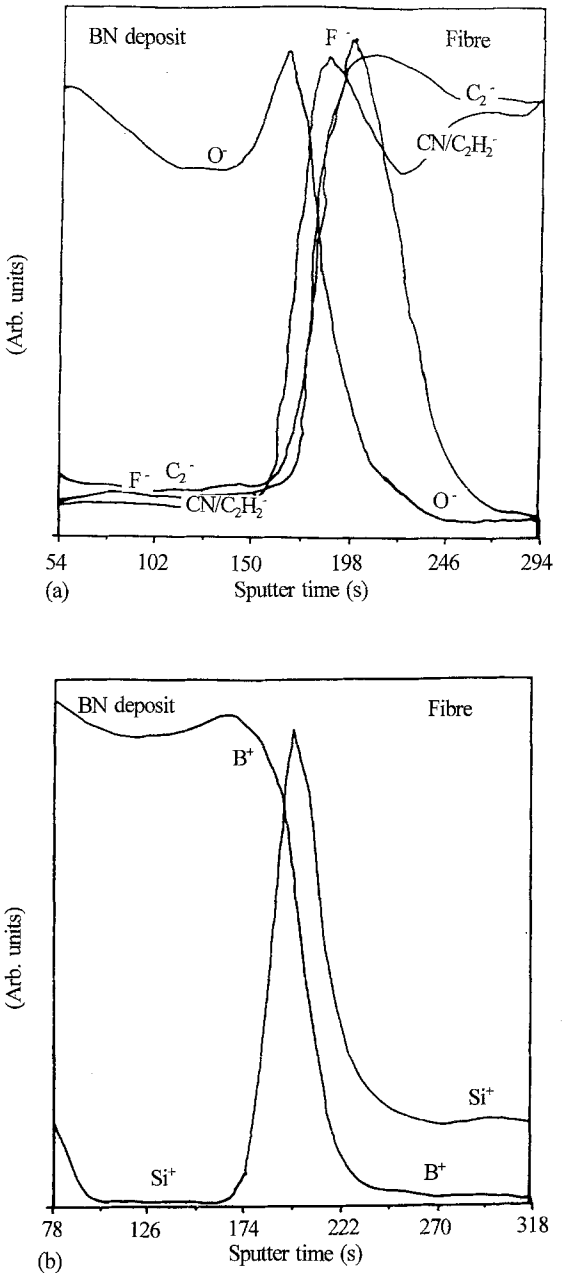

Figure 4 SIMS depth profile analysis of the BN interphase deposited by CVI (infiltration time 20 h) from a BF_3–NH_3 precursor, on an ex-PCS fibre: (a) negative ions, and (b) positive ions.

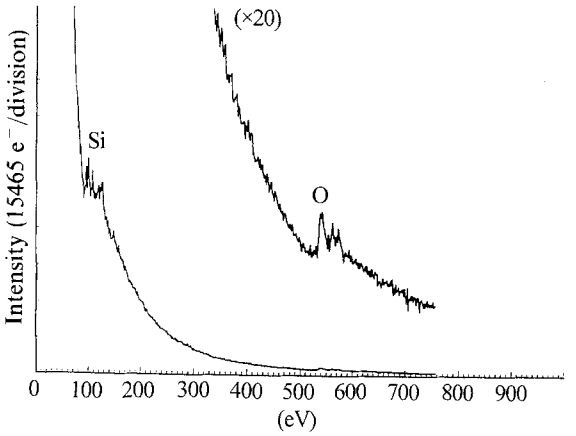

Figure 5 EELS spectrum recorded at the BN/fibre interface from an ex-PCS fibre coated by BN deposited by CVI (infiltration time 20 h) from a BF_3–NH_3 precursor.

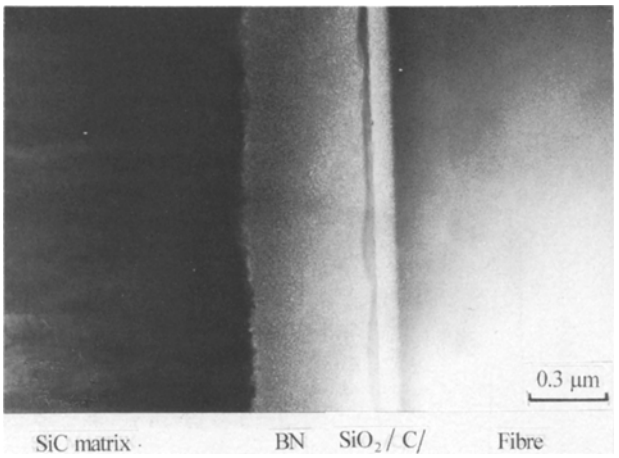

Figure 6 Transmission electron micrograph of the fibre/matrix interfacial zone in a 2D-SiC (ex-PCS)/BN/SiC (CVI) composite prepared according to the ICVI process.

spacing, derived from the TEM characterization (EELS and SAD data), of the BN interphase after the second CVI step (i.e. in the 2D-SiC/BN/SiC composite) are shown in Table I. From a comparison with the data corresponding to the material after the first CVI step, it clearly appears that the infiltration of the CVI/SiC matrix results in the following change in the BN interphase: (i) the N/B atomic ratio tends towards that corresponding to stoichiometric BN, (ii) the amount of oxygen is significantly lower, and (iii) the d_{002} interlayer spacing slightly decreases.

In fact, the BN interphase still has a turbostratic character (the d_{002} interlayer value, 0.351 nm, still being far from that, 0.333 nm, corresponding to hex-BN well-ordered three-dimensionally). Furthermore, its microtexture, as shown in Fig. 7, is very similar to that observed in the deposit immediately after the first CVI step (Fig. 1a). In the majority of the material, the BN layers are randomly orientated except in the very vicinity of the silica substrate (i.e. over a thickness of the order of 10 nm) where they tend to be aligned parallel to the substrate surface [30].

3.2.2. The BN/SiC matrix interface

On the basis of the SAD patterns (Fig. 8b), the SiC matrix deposited from CH_3SiCl_3/H_2 consists mainly of microcrystals of the cubic β-modification (blende type). However, it is known that such deposits also contain significant amounts of hexagonal polytypes [35]. No attempt was made to characterize in a detailed manner the SiC matrix structure, the emphasis of the present work being on the characterization of the fibre–matrix interfacial zone.

As is apparent from the TEM bright-field image shown in Fig. 8a, no extended interaction zone (which could have resulted from interdiffusion phenomena during the long CVI treatment at 1000 °C) is observed at the BN/SiC (CVI) interface. This result suggests that the BN coated ex-PCS SiC fibres are a chemically inert substrate with respect to the gas phase involved in the CVI of SiC from a CH_3SiCl_3/H_2 precursor. In fact, this conclusion is consistent with the results

TABLE I Chemical analysis and interlayer spacing of BN interphases

Samples	N/B atomic ratio (EELS)	Oxygen (at %)	d_{002} (nm)
BN interphase as-infiltrated	0.7–0.8	10–15	0.365
BN interphase in the SiC/BN/SiC composite	0.9–1.0	< 5	0.351
BN interphase infiltrated in a carbon felt and annealed (20 min, 1200 °C, vacuum)	0.9–1.0	< 6	0.357

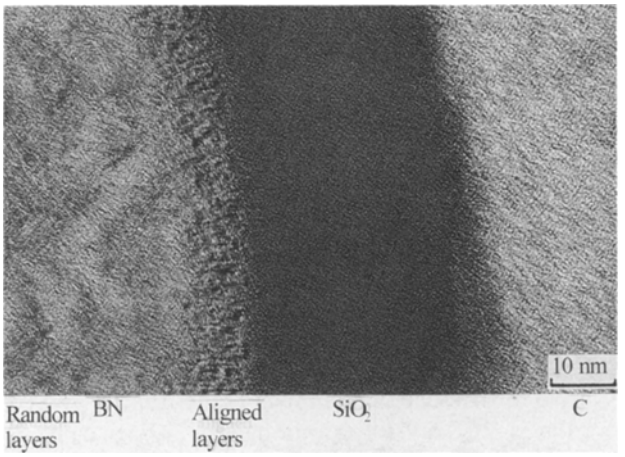

Figure 7 TEM bright-field image of the transition zone between the BN interphase and the silica sublayer in a 2D-SiC (ex-PCS)/BN/SiC (CVI) composite.

of thermodynamic calculations (performed for a CH_3SiCl_3/H_2–BN system under conditions simulating the second CVI step considered here), according to which neither B_4C nor Si_3N_4 (the solid phases which might have resulted from a chemical reaction between SiC and BN) are present at equilibrium at 1000 °C [36].

3.2.3. The BN/fibre interface

As already mentioned, the interfacial zone between BN and the ex-PCS SiC fibre is much more complex. It is apparent from the TEM image shown in Fig. 6, that this interfacial zone consists of two well-defined sublayers: one, in contact with the BN-interphase, has a somewhat irregular border on the BN-side and a mean thickness of 40 nm, whereas the other, adjacent to the fibre, is more regular with a mean thickness of about 80 nm. On the basis of the EELS spectra shown in Fig. 9, the former was identified with silica (not pure but containing some boron) and the latter with carbon. Both were observed to be amorphous (from electron diffraction patterns). Furthermore, the shape of the carbon C *K* EELS peak is characteristic of a carbon with a low state of organization [37, 38].

The occurrence of the silica and carbon sublayers at the BN/fibre interface is confirmed by the AES concentration depth profiles recorded from a failure surface of a 2D-SiC/BN/SiC composite loaded in flexion (Fig. 10). Starting from the failure surface (which seems

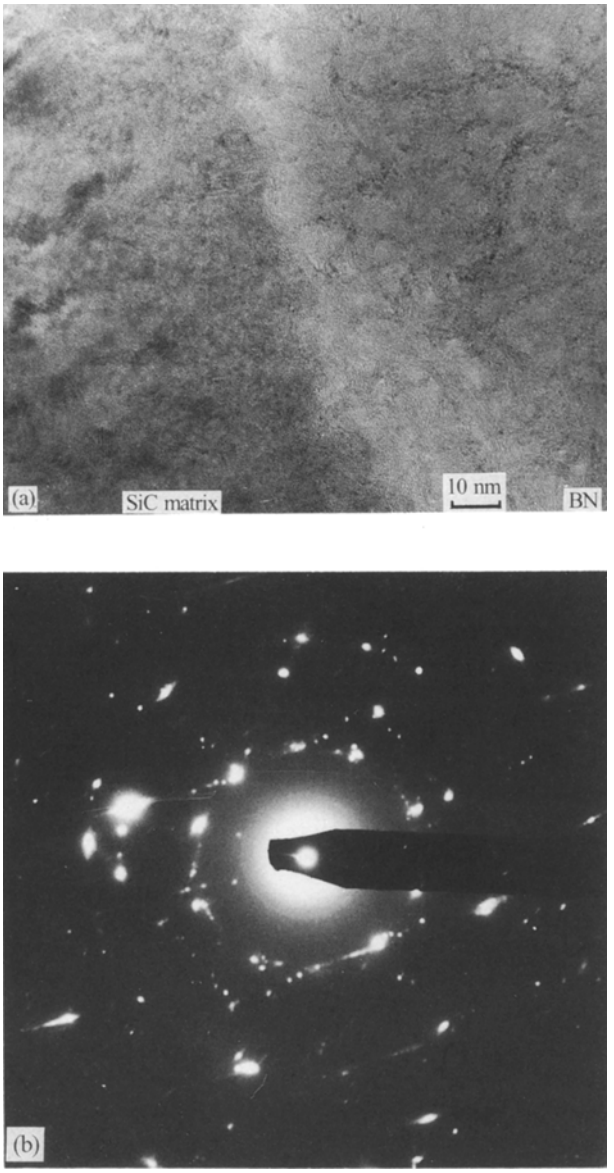

Figure 8 TEM analysis of a 2D-SiC (ex-PCS)/BN/SiC (CVI) composite in the vicinity of the BN/SiC (CVI) interface: (a) bright-field image of the interface, and (b) SAD pattern of the SiC (CVI) matrix.

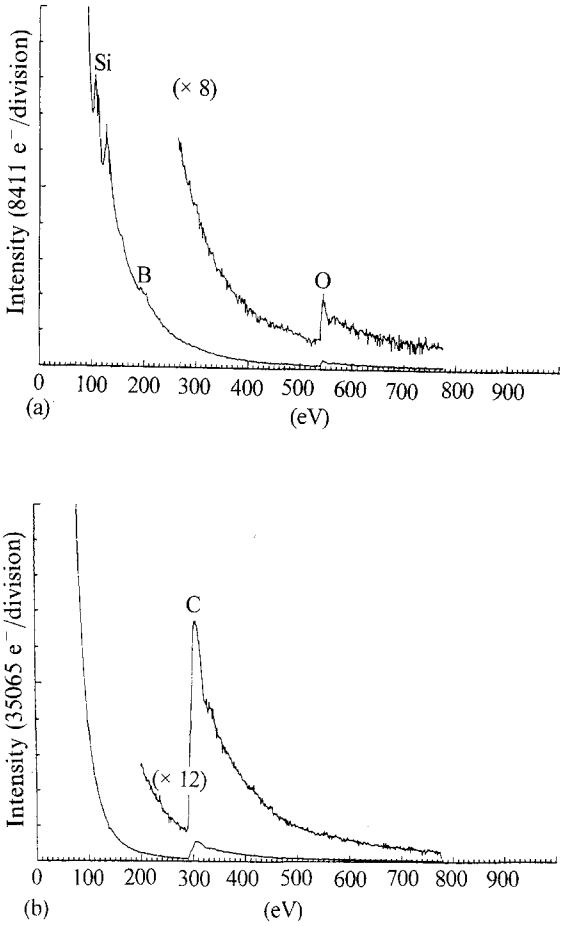

Figure 9 EELS spectra of the BN/fibre interfacial zone in a 2D-SiC (ex-PCS)/BN/SiC (CVI) composite: (a) silica sublayer, and (b) carbon sublayer.

to be located within the BN interphase but in the immediate vicinity of the BN/SiO_2 interface), the silica sublayer (sputtering times 1–8 min) and then the carbon sublayer (sputtering times 8–16 min) are successively observed. Finally, there seems to be a smooth transition (i.e. a carbon-enriched transition zone) between the carbon sublayer and the bulk of the SiC ex-PCS fibre (average composition 57 at % Si, 30 at % C and 12 at % O [39]). It is worthy of note that some overlapping seems to occur among the sublayers (e.g. BN/SiO_2 or SiO_2/C). This feature does not necessarily mean that interdiffusion phenomena took place between the sublayers. It could also be the result of artefacts related to, for example, the curvature of the surface (the diameter of an ex-PCS SiC fibre is typically 15 μm) or different sputtering rates enhancing the microrelief of the sputtered surfaces.

3.2.4. Intrinsic thermal evolution of ex-PCS SiC fibres

In order to assess the origin of the silica and carbon sublayers observed at the BN–fibre interface, i.e. to establish whether their formation could be related to the chemistry of the BN and/or SiC CVI, on the one hand, or more simply to some thermal evolution of the fibre itself, on the other, AES concentration depth profiles were recorded from ex-PCS SiC fibres which have been submitted to each of the two thermal treatments defined in Section 2.1. The results are shown in Figs 11 and 12.

The surface of an ex-PCS SiC fibre submitted to heat treatment 1 is made of silicon, carbon and oxygen atoms, as is apparent from Fig. 11a. The kinetic energy of the Auger electrons corresponding to the Si_{LVV} transition is observed to be of about 79 eV, a value which is not too far from that reported for silica (76 eV) (whereas that for SiC is 92 eV) [31–33]. Furthermore, the concentration depth profiles recorded along a direction perpendicular to the fibre surface (the origin being on the fibre surface itself) show successively: (i) a carbon-rich zone (sputter times less than 10 min) which could be due either to some contamination of the sample by both the annealing furnace and AES apparatus or to the pyrolysis of the fibre organic size, and (ii) a maximum in both the silicon and oxygen profiles (sputtering time of about 12 min) which suggests that some silica might have been formed (Fig. 11b). Finally, both boron and nitrogen are observed in small amounts near the fibre surface (sputtering times less than 15 min), probably

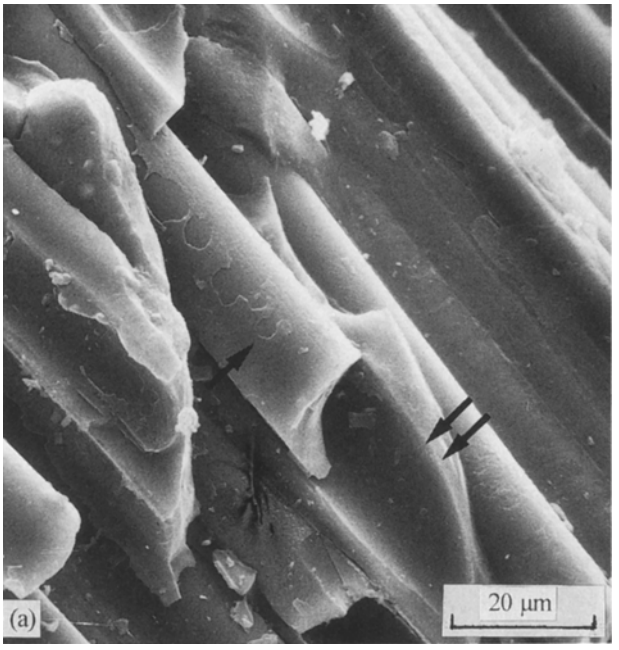

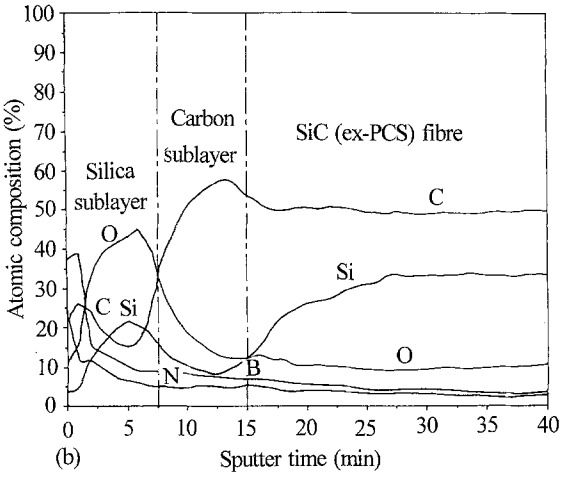

Figure 10 Analysis of the BN/fibre interfacial zone of a 2D-SiC (ex-PCS)/BN/SiC (CVI) composite: (a) failure surface as observed by scanning electron microscopy after a bending test (single arrow, silica sublayer; double arrow, BN interphase), (b) AES depth profile perpendicular to the surface of a fibre extracted from the composite.

originating from an outgasing of BF_3 and NH_3 adsorbed (as BF_x NH_y species) on the cold surface of the BN furnace in which heat treatment 1 was performed [28].

The AES analysis performed on a fibre submitted to heat treatment 2 (Fig. 12) confirms the features already mentioned for the fibre submitted to heat treatment 1, i.e. a well-defined carbon/SiO_2 carbon sequence near the fibre surface. Moreover, the concentration depth profiles are very similar to those observed for the 2D-SiC/BN/SiC composites (Fig. 10b).

3.3. Deflection of microcracks at the fibre–matrix interfacial zone

The samples observed by TEM have been submitted to various stress fields during the preparation of the thin foils, which result in microcracking. In a few

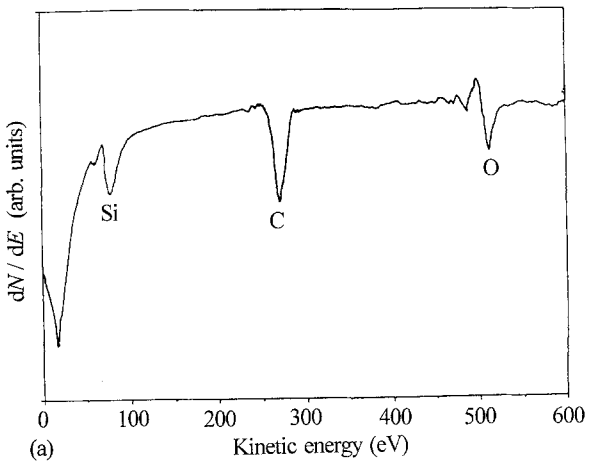

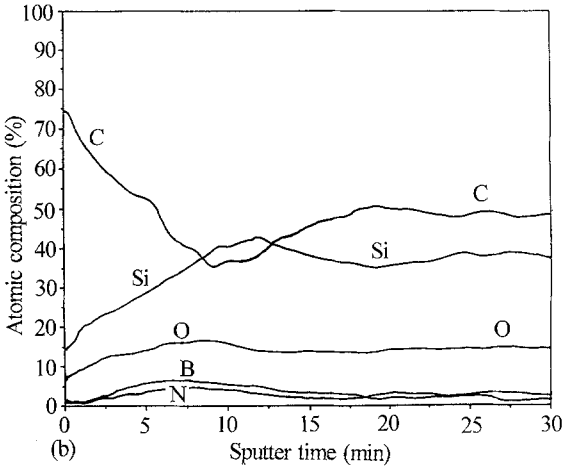

Figure 11 AES analysis of an ex-PCS fibre submitted to heat treatment 1 (1000 °C): (a) AES spectrum of the fibre surface recorded to the d[$N(E)$]/dE mode; (b) concentration–depth profile perpendicular to the surface of the fibre.

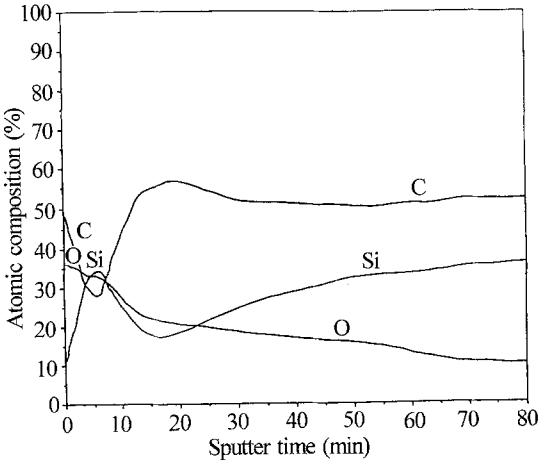

Figure 12 AES concentration–depth profile of an ex-PCS SiC fibre submitted to heat treatment 2 (864 h annealing at 1000 °C) along a direction perpendicular to the fibre surface.

cases, those microcracks could be characterized. As an example, Fig. 13a shows a microcrack which has been initiated in the SiC matrix where it has propagated in Mode I (i.e. roughly perpendicular to the fibre axis). Then, it propagated through the BN interphase along a slightly more irregular path before being deflected in Mode II at the BN/silica interface. As a result, a

decohesion of the interface took place over more than 1.5 μm, whereas, in the opposite direction, local decohesion areas are also observed.

In the other example shown in Fig. 13b, a microcrack, after having crossed the interfacial zone (i.e. the BN interphase and both the SiO_2 and carbon sublayers) has induced the failure of the fibre itself where it propagated in Mode I. All these features are consistent with the modern concepts of the failure modes, at the submicrometre scale, of tough CMCs and can be considered as one of the first experimental proofs of the ability of a fibre/matrix interface to arrest and/or deflect in Mode II, the microcracks originating from the early failure of a brittle matrix.

4. Discussion

The experimental results which have been presented in Section 3 can be used to discuss some key points related to the processing and micromechanical behaviour of SiC/BN/SiC composites.

4.1. Nature and thermal evolution of the BN interphase

The data presented in Section 3.1.2 clearly show that the coating, deposited on the fibres within the open porosity of a 2D-ex-PCS SiC preform, from a BF_3–NH_3 precursor at 1000 °C and under reduced pressure (ICVI conditions), is made of turbostratic non-stoichiometric boron nitride and contains significant amounts of oxygen.

During the long SiC CVI treatment, which is necessary to fill as completely as possible the preform porosity by SiC, i.e. several hundreds of hours at about 1000 °C, several important changes occur in the BN interphase: (i) it becomes almost stoichiometric, and (ii) the oxygen concentration is divided by a factor of three. On the other hand, from a structural point of view, the material remains turbostratic owing to the fact that the annealing treatment took place at too low a temperature to result in any three-dimensional ordering of the layered structure.

These features are consistent with the results previously published by several authors on the CVD of BN from various precursors. As an example, Matsuda and co-workers [40, 41] as well as Marchand *et al.* [42] have established very recently that BN prepared from BCl_3–NH_3 precursors tends to become crystalline only when it is deposited or annealed beyond about 1800 °C. For lower deposition temperatures, i.e. 800 °C < T < 1400 °C, their BN deposits were also non-stoichiometric and contaminated by oxygen. Conversely, for higher deposition or annealing temperatures (T > 1400 °C), the BN deposits tended towards stoichiometric and contained less oxygen, a feature which could be explained by the evolution of gaseous boron oxides.

The principle of the CVI process in fact precludes the use of high infiltration temperatures [27, 43]. Therefore, the BN interphase infiltrated in a fibre preform by ICVI from any gaseous precursor (including BF_3–NH_3 and BCl_3–NH_3) would consist of defective boron nitride. However, it is fortunate that some of the defects initially present in the as-deposited material (i.e. lack of stoichiometry, oxygen impurity) are eliminated during the long duration of the SiC CVI step. Finally, and as already mentioned, the BN-interphase has many structural and microstructural features in common with the pyrocarbon interphase deposited from, for example, CH_4 under similar conditions.

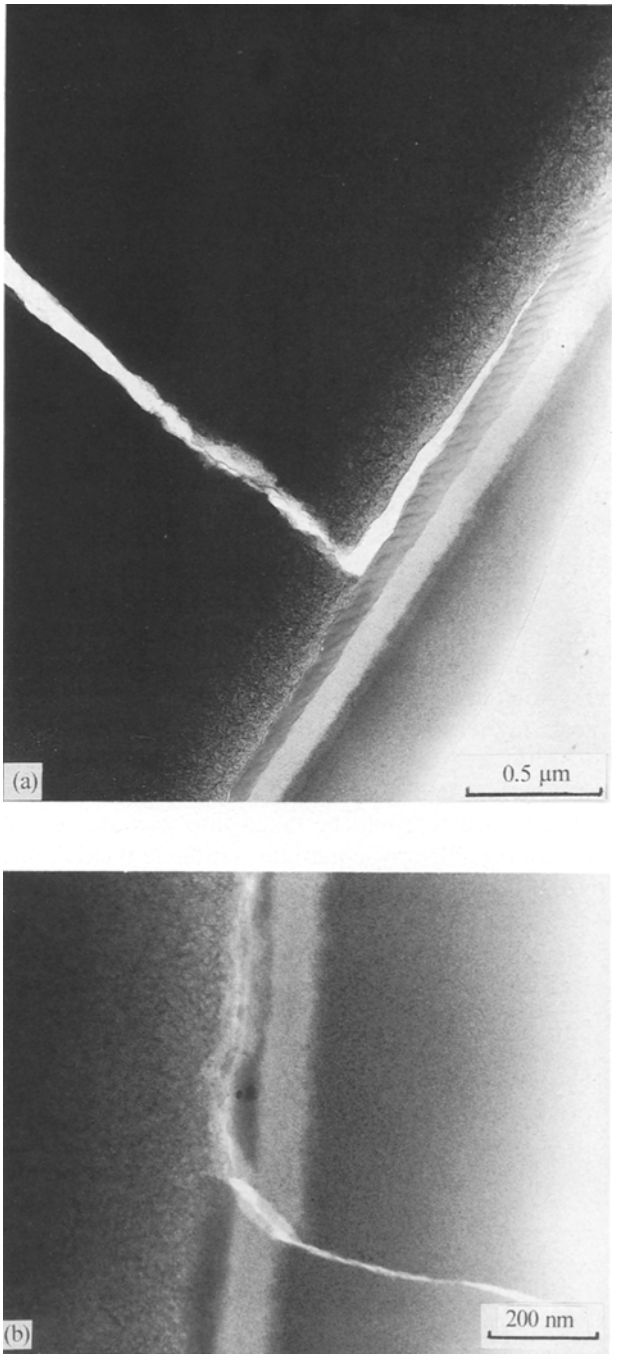

Figure 13 TEM analysis of the interaction between a microcrack and the fibre/matrix interfacial zone in a thin foil of 2D-SiC/BN/SiC composites: (a) deflection in Mode II of a microcrack at the BN/SiO_2 interface; (b) fibre failure in Mode I due to a microcrack which has been first deflected in Mode II at the BN/SiO_2 interface.

4.2. Chemical compatibility of the BN interphase with ex-PCS SiC fibres and SiC CVI matrix

At the beginning of the CVI step 1, the ex-PCS SiC

fibres are exposed at about 1000 °C to the BF_3–NH_3 gas phase. An important question is to know whether or not the fibrous substrate is chemically compatible with such a gas phase, a negative answer indicating that the fibres would be chemically surface damaged and thus would loose part of their reinforcing potential.

This subject has been studied on the basis of a thermodynamic approach and the results discussed in detail elsewhere [34]. It will be sufficient to recall here the main conclusions in order to give a theoretical frame to the discussion of the present experimental results. Substrates of either pure carbon or silica can be considered as quasi-unreactive with respect to the BF_3–NH_3 precursor, for $1 < \alpha < 15$ (with $\alpha = NH_3/BF_3$ mole ratio) and 850 °C $< T <$ 1450 °C, the deposition reaction corresponding in a first approximation, to the following equation

$$BF_{3(g)} + NH_{3(g)} \rightleftharpoons BN_{(s)} + 3HF_{(g)} \quad (1)$$

Under such conditions, deposition takes place with a very low conversion yield, i.e. less than 20% in the most favourable case. Conversely, pure SiC or SiC/SiO_2 hybrid substrates are very reactive, the deposition mechanism involving a chemical attack of the substrate which could be taken into account on the basis of the following equations written in the case of a pure SiC substrate material

$$\frac{4}{3}BF_{3(g)} + \frac{4}{3}NH_{3(g)} \rightarrow \frac{4}{3}BN_{(s)} + 4HF_{(g)} \quad (1)$$

$$4HF_{(g)} + SiC_{(s)} \rightarrow C_{(s)} + SiF_{4(g)} + 2H_{2(g)} \quad (2)$$

$$NH_{3(g)} + \frac{3}{4}SiC_{(s)} \rightarrow \frac{1}{4}Si_3N_{4(s)} + \frac{3}{4}C_{(s)} + \frac{3}{2}H_{2(g)} \quad (3)$$

$$2NH_{3(g)} \rightarrow N_{2(g)} + 3H_{2(g)} \quad (4)$$

$$\frac{4}{3}BF_{3(g)} + \frac{13}{3}NH_{3(g)} + \frac{7}{4}SiC_{(s)} \rightarrow \frac{4}{3}BN_{(s)} + \frac{7}{4}C_{(s)} + \frac{1}{4}Si_3N_{4(s)} + SiF_{4(g)} + \frac{13}{2}H_{2(g)} + N_{2(g)} \quad (5)$$

Under such conditions, i.e. when NH_3 is in excess, (i) the SiC substrate is chemically attacked by both source species and BN is observed to be mixed (at least at the very beginning of the deposition process) with carbon and silicon nitride, and (ii) the conversion of BF_3 into BN is quasi-quantitative. Finally, when the hybrid SiC/SiO_2 substrate is used instead of pure SiC, $Si_2N_2O_{(s)}$ is also formed.

The experimental results which have been presented in Section 3 support the assumption that a preform made of ex-PCS SiC fibres can be considered as quasi-unreactive with respect to the BF_3–NH_3 precursor, although the fibres are a mixture of SiC + C + Si–(C,O) which should be reactive. In fact, the surface analysis which has been done on ex-PCS fibres submitted to heat treatment 1 (simulating the transient phase which takes place immediately before the BF_3–NH_3 precursor is allowed to flow over the substrate heated at 1000 °C) suggests that the fibre surface consists of a sequence (or a mixture) of carbon and silica (Fig. 11b), both being unreactive as established by the thermodynamic calculations.

The conclusion drawn here concerning the nature of the surface of the ex-PCS SiC fibres is consistent with the results of the ESCA and AES analyses performed by Macey *et al.* [44] or Porte and Sartre [45] on desized fibres. Furthermore, Maniette [8] has concluded, on the basis of TEM analyses conducted on fibres submitted to a thermal cycle similar to our thermal treatment 1, that the fibre surface consisted of a layer of silica overcoated with a very thin film of carbon.

It thus appears that the C + SiO_2 coating protects the reactive ex-PCS SiC fibres against a chemical attack from the BF_3–NH_3 precursor at 1000 °C, as suggested by the smooth surface of the fibre partly debonded from the BN interphase, shown in Fig. 2a. On the other hand, the cavities present along the imprint left by a fibre in the BN interphase (Fig. 2b) suggest that chemical phenomena involving a gas evolution (i.e. bubbles) did take place in the vicinity of the fibre/interface. This latter topic will be discussed in Section 4.3.

In a similar way, the analysis of the BN/SiC (CVI) matrix interface (Fig. 8a) suggests that no reaction took place between the BN-infiltrated preform and the gas phase (i.e. CH_3SiCl_3/H_2 mixtures, with $H_2/CH_3SiCl_3 > 1$) used for the infiltration of the SiC matrix. In order to justify this assumption, thermodynamic calculations were performed, according to a procedure which has been published elsewhere [26–27], in the CH_3SiCl_3/H_2–BN system, for the following conditions: (i) initial composition $[CH_3SiCl_3]_{in} = 1$ mol; $< BN >_{in} = 1$ mol; $\alpha = [H_2]_{in}/[CH_3SiCl_3]_{in}$ ranging from 0–50, and (ii) $T = 1300$ K and $P = 1$ kPa [37, 38]. The results, shown in Fig. 14, clearly established that no reaction occurs between BN and the gas phase.

4.3. Effect of the SiC CVI step on the SiC (ex-PCS) fibres

The experimental results reported in Section 3 strongly support the assumption that the carbon/silica sequence, observed in the interfacial zone between the ex-PCS SiC fibre and the BN interphase, in the 2D-SiC/BN/SiC composites, has been formed during the long SiC CVI step 2 at 1000 °C, acting as an annealing treatment. In fact, this sequence cannot be the result of a chemical reaction between the fibre and the gas phase during the deposition of BN because it has been established in Section 4.2 that (i) some carbon and silica are both already present at the fibre surface when the BF_3–NH_3 precursor is allowed to flow over the substrate, and (ii) under such conditions the fibrous preform is a quasi-unreactive substrate. On the other hand, carbon and silica, which are present only in small amounts at the beginning of the SiC CVI step 1, are observed as well-identified sublayers at the end of the SiC CVI step 2, their thicknesses being of about

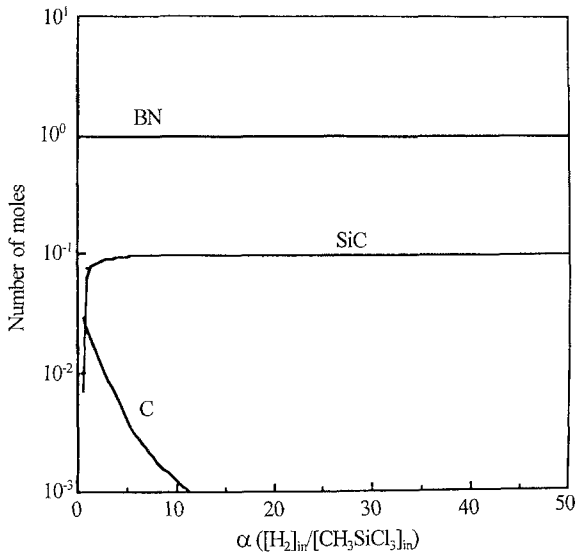

Figure 14 Thermodynamical calculations of the formation of SiC from a CH_3SiCl_3–H_2 precursor in presence of BN for $T = 1300$ K, $P = 1$ kPa, $[CH_3SiCl_3]_{in} = 0.1$ mol, $< BN >_{in} = 1$ mol.

40 and 80 nm for silica and carbon, respectively (Figs. 6, 9 and 10b). Finally, a pure annealing treatment performed at 1000 °C under vacuum for several hundreds of hours (i.e. under thermal conditions quite similar to those seen by the fibres during SiC CVI step 2) has also yielded a similar carbon–silica sequence at the fibre/BN interphase (Fig. 12). Therefore, the experimental data presented here clearly establish that the extension of carbon and silica sublayers present at the fibre/BN interface are a direct consequence of the specific features of the ICVI process used to infiltrate the SiC matrix in the porous 2D-SiC (ex-PCS) preform (that process acting as a long annealing treatment with respect to the thermodynamically unstable SiC (ex-PCS) fibres).

The carbon–silica double layer present in 2D-SiC/BN/SiC composites, which results mainly from the thermal evolution of the ex-PCS fibres as already discussed, has nevertheless some features which are directly related to the chemistry of the CVI processing technique. Both the carbon and silica sublayers in fact contain small amounts of impurity atoms which originate from the CVI 1 and/or 2 steps. The carbon sublayer, which is amorphous does not seem to contain significant amounts of foreign atoms, including nitrogen, on the basis of the EELS data (Fig. 9b). This remark may be used to justify a posteriori the assignment of the ions of mass 26 to $C_2H_2^-$ (rather than to CN^-) which has been done in the analysis of the SIMS spectra reported in Section 3.1.2, assuming that hydrogen is present in the carbon sublayer at least in small amounts (Fig. 4a). This hydrogen could originate either from the fibre where its bulk concentration is known to be of the order of 0.2 wt% according to Ichikawa *et al.* [46], or from the CVI process gas phase. Furthermore, the interfacial carbon sublayer might also contain some fluorine (i.e. probably less than 1 at %) introduced in the material during the infiltration of BN (Fig. 4a). In a similar way, the EELS analysis has shown that the silica sublayer, which is adjacent to the BN interphase, contains boron (Fig. 9a). In fact, BN is often used as a boron source for doping both silicon and silica [47–48]. Boron might have diffused in the solid state in silica during the long SiC CVI step at 1000 °C giving rise to a boria–silica glass known to exhibit a lower glass transition than that of pure silica. Therefore this glass might be a better encapsulating material for the fibre, at the CVI processing temperature (i.e. about 1000 °C).

As already mentioned, the formation of a carbon–silica double layer at the fibre surface is part of the complex phenomena that take place when an ex-PCS fibre is annealed above 1000 °C under vacuum or inert atmosphere. Such phenomena have been studied by several authors [7, 8, 49–53] but only a few of them mentioned that the C/SiO_2 sequence is the result of the thermal degradation of the fibre [8, 49, 53]. According to the model proposed recently by Laffon *et al.* [24], ex-PCS SiC fibres consist of a continuum of SiC_4 and SiC_xO_y (with $x + y = 4$) tetrahedral species, in which nanometre-scale domains of pure SiC_4 tetrahedra are separated from one another by amorphous zones of silicon oxycarbide. Furthermore, nanometre-scale aggregates of aromatic carbon (still partly bonded to hydrogen atoms) are inserted in the continuum. Obviously, this nanostructure which is a remnant of the organic state, is not stable at high temperatures, from a thermodynamic point of view [51]. As a result, when such a metastable fibre is annealed, the following phenomena are thought to take place: (i) a decomposition of the Si–(C,O) ternary species giving rise to an evolution of both SiO and CO (this decomposition starts near the fibre surface and then moves towards the fibre core), and (ii) a coarsening of the SiC domains in that zone where the decomposition of the Si–(C,O) phase already took place (the SiC domains being no longer isolated). It is thought that the formation of the carbon–silica double layer at the fibre surface is directly related to (i).

It clearly appears from the model presented above that the thermal degradation of ex-PCS fibres and consequently the formation of the C/SiO_2 layer is thermally activated and depends on time. Therefore, it is not surprising that it is observed to take place during the long annealing treatment at 1000 °C experienced by the fibres during the SiC ICVI processing step. The same arguments could be used to explain the origin of the carbon (silica) layer observed at the interface between such a fibre and a glass–ceramic matrix in composites processed by hot pressing. In this latter case, the thermal treatment is much shorter but the temperature is higher (i.e. 1200–1300 °C) [54–56].

Finally, the microcavities which have been observed (Fig. 2b) along the imprint left by a fibre in the BN interphase, could have been formed during the CVI processing of the composites, by bubbles of gas (of CO and/or SiO) resulting from the thermal decomposition of the ex-PCS fibres and which were trapped at the interface.

4.4. Interaction between the fibre–matrix interfacial zone and microcracks generated in the brittle SiC matrix

When a composite made of continuous ceramic fibres

embedded in a ceramic matrix is loaded, e.g. in tension along the fibre direction, the brittle matrix fails first, generating numerous microcracks propagating in Mode I. The mechanical behaviour of the composites, particularly its failure mode and toughness, depends on the nature of the interaction occurring between these microcracks and the fibre/matrix interfaces [1–3]. When the fibres are strongly bonded to the matrix, which is the case for many CMCs, the notch effects arising from the matrix microcracking result in the early failure of the fibres (i.e. a crack propagating in Mode I in the matrix is not arrested by interface). Under such conditions, CMCs behave as brittle materials. Conversely when the fibres are only weakly bonded to the matrix, the fibre/matrix interfacial zone either acts as a crack arrester or deflects the crack in Mode II, debonding the fibre from the matrix over a certain length. Under such conditions, (i) the matrix microcracking no longer results in the early failure of the fibre, (ii) the fibre can be loaded up to its intrinsic failure strain, and (iii) numerous damaging phenomena occur which increase the toughness of the material.

Up to now, it was admitted that an efficient way to control properly the fibre–matrix coupling was to insert a thin interphase of, for example, pyrocarbon between the two components. In glass–ceramic matrix composites reinforced with ex-PCS SiC fibres, we have suggested in Section 4.3 that the carbon interphase might result from a surface decomposition of the fibres taking place during the processing of the composites (which consists usually of a hot-pressing step at 1200–1300 °C followed by an annealing treatment at about 1000 °C to ceram the glass matrix). Under such processing conditions, the materials are tough and a carbon/silica sequence is observed at the fibre/matrix interface [54–56]. Conversely, when such composites are processed according to a low-temperature route (e.g. sol–gel), they exhibit a brittle behaviour [57]. This difference of failure mode is probably related to the fact that, in the latter case, temperature was too low to give rise to any significant decomposition of the fibres (therefore no carbon (silica) interfacial zone was formed).

As shown in Fig. 13, a similar deflection of the microcracks arising from the failure of the SiC CVI matrix is observed within the fibre/matrix interfacial zone in the 2D-SiC/BN/SiC composites studied here. However, crack deflection does not occur within the BN interphase, as it could be expected, but rather at the interface between boron nitride and the silica thin layer resulting from the thermal decomposition of the ex-PCS fibre. This feature suggests that the BN/SiO_2 interface might be the weaker link in the interfacial phase sequence (i.e. SiC CVI matrix/BN/SiO_2/C/ex-PCS SiC fibre).

The low adhesion between BN and silica, clearly apparent from Fig. 2a, might have various origins, including (i) the lack of strong interactions between both layers during processing (which precluded a bonding by diffusion), (ii) the fact that the BN layers are deposited, at the very beginning of the process, almost parallel to the fibre surface (a well-known feature of the CVD of layered structure materials) (Fig. 7), and (iii) the strong anisotropy of the coefficient of thermal expansion (CTE) of boron nitride, i.e. $\alpha_c = 40.5\ 10^{-6}\,°C^{-1}$ and $\alpha_a = 0$ at 770 °C, according to Pease and mentioned in [58]. Features (ii) and (iii) might well be the most important. Feature (ii) when taken alone suggests that the shear strength of the interfacial zone could be controlled by the very weak chemical bond (Van der Waals type) between two adjacent BN layers turbostratically stacked (bond length 0.35 nm, as shown in Table I). Furthermore, when (iii) is added to (ii) one might even conclude that the contraction of the BN interphase during cooling from 1000 °C to room temperature could either leave the interphase in tension or already debond the interphase from the fibre. It is noteworthy that Sinclair and Simmons [58] mentioned, in their study of BN/Sialon particulate composites, that the boundaries between the two phases were often separated when the interface involves the basal plane of BN but rarely when the contact was between the edges of a BN plate and Sialon. On the basis of the similarity between turbostratic BN and pyrocarbon, the same arguments could be applied to the SiC CVI matrix/pyrocarbon/SiO_2/C/ex-PCS SiC fibres sequence.

In a recent article, Rawlins *et al.* [7] have correlated the lack of reproducibility of the mechanical properties between specimens of SiC (ex-PCS)/SiC (CVI) composites prepared by forced-CVI, on the one hand, and the occurrence, or not, of an interfacial zone consisting of two amorphous sublayers (one of which, i.e. the thicker, being assigned to silica), on the other hand. Pull-out was observed when the interfacial film was present and was still enhanced when a pyrocarbon interphase was deposited on the fibre prior to the FCVI step. On the contrary, no pull-out occurred in the other case [7]. These results are consistent with the conclusions of the above discussions. In the FCVI process, the deposition rate is much faster than in the ICVI process used in the present work. As a result, the ex-PCS metastable fibres are submitted to a less severe annealing (20–40 h at 1100–1200 °C in FCVI instead of several hundreds of hours at about 1000 °C in ICVI [28, 42, 59, 60]. Under such conditions, the interfacial zone could have been not extended enough to allow (i) the assignment of the other sublayer (probably carbon), and (ii) crack deflection and pull-out. The role played by the pyrocarbon interphase is obviously very similar to that of BN as already mentioned. Finally, the authors reported that no pull-out occurred with, consequently, a brittle failure mode, when the pyrocarbon-layered interphase was replaced by an isotropic silicon interphase, which is consistent with the present discussion (inasmuch as such interphase material could be assumed to be strongly bonded to the silica interfacial layer).

5. Conclusions

A detailed analysis by TEM, AES and SIMS of the fibre–matrix interfacial zone generated during the processing of SiC/BN/SiC composites by CVI, has led to the following conclusions.

1. The submicrometre BN interphase is made of turbostratic BN, almost stoichiometric (N/B = 0.9–1.0) and containing less than 5 at% oxygen.

2. During the long infiltration step of the SiC matrix at 1000 °C, the ex-PCS SiC fibres undergo some decomposition, resulting in the growth of an SiO_2/C amorphous double layer at the BN/fibre interface.

3. Microcracks arising from the failure of the brittle SiC matrix are deflected at the BN/SiO_2 interface, thought to be the weaker link in the interfacial SiC CVI matrix/BN interphase/SiO_2/C/ex-PCS SiC fibre sequence.

4. Therefore, the combination of a layered structure interphase (either pyrocarbon or boron nitride) and the products (i.e. silica and carbon) resulting from the thermal decomposition of the ex-PCS SiC fibres is thought to be responsible for the toughness of the SiC/SiC composites processed by ICVI.

Acknowledgements

This work was supported by the French Ministry of Research and the Société Européenne de Propulsion (SEP) through a thesis fellowship. The assistance of SEP and Science et Surface, respectively, in the SiC infiltration and SIMS analyses, is acknowledged.

References

1. J. AVESTON, G. A. COOPER and A. KELLY, in Proceedings of the Conference "The Properties of Fibre Composites", National Physical Laboratory, Teddington, (IPC Science and Technology Press, London 1971) paper 1 p. 15.
2. D. B. MARSHALL and A. G. EVANS, *J. Amer. Ceram. Soc.* **68** [5](1985) 225.
3. R. NASLAIN, *J. de Phys. Coll.* **C1**, suppl. 2,47 (1986) C1–703.
4. J. G. THEBAULT, Fr. Pat. 2567 874, 20 July, 1984.
5. R. W. RICE, U. S. Pat. 4642 271, 10 February, 1987.
6. L. GRATEAU, N. LOB and M. PARLIER, in "International Conference" Canterbury, UK, Vol. 14, "Science of Ceramics" edited by D. Taylor (Institute of Ceramics, 1987) p. 885.
7. M. H. RAWLINS, T. A. NOLAN, D. P. STINTON and R. A. LOWDEN, in "Proceedings of MRS Symposium on Advanced Structural Ceramics", Vol. 78, edited by P. F. Becher, M. V. Swain and S. Sõmiya, (MRS, Pittsburg, PA 1986) p. 223.
8. Y. MANIETTE, Thesis, University of Pau (1988).
9. E. MENESSIER, A. GUETTE, R. PAILLER, R. NASLAIN, L. RABARDEL, B. HOSTEN. T. MACKE and P. LESPADE, in "Proceedings of ECCM 3", Bordeaux 1989 edited by A. R. Bunsell, P. Lamicq and A. Massiah, (Elsevier Applied Science, London, New York, 1989) p. 121.
10. O. DUGNE, S. PROUHET, A. GUETTE, R. NASLAIN and J. SEVELY, *ibid.*, p. 129.
11. B. BENDER, A. SHADWELL, C. BULIK, L. INCOVARTI and D. LEWIS, *Amer. Ceram. Soc. Bull.* **65** (1986) 363.
12. D. P. PARTLOW, *Adv. Ceram. Mater.* **3** (1988) 553.
13. R. N. SINGH and M. K. BRUN, *Adv. Ceram.* **3** (1988) 235.
14. V. A. LAVRENKO and A. F. ALEXEEV, *Ceram. Int.* **12** (1988) 235.
15. G. LACRAMBE, Thesis, University of Bordeaux I (1988).
16. H. HANNACHE, R. NASLAIN and C. BERNARD, *J. Less-Common Metals* **95** (1983) 221.
17. H. HANNACHE, J. M. QUENISSET, R. NASLAIN and L. HERAUD, *J. Mater. Sci.* **19** (1984) 202.
18. H. O. PIERSON, *J. Compos. Mater.* **9** (1975) 828.
19. R. N. SINGH, in "Proceedings of the 10th International Conference on CVD", Honolulu, edited by G. W. Cullen (The Electrochemical Society, Princeton, NJ, 1987) p. 543.
20. J. J. GEBHART, in "Proceedings of the 4th International Conference on CVD", Boston (The Electrochemical Soceity, Princeton, NJ, 1973) p. 460 (extended abstract).
21. B. A. BENDER, R. W. RICE and J. R. SPANN, *Ceram. Engng. Sci. Proc.* **6** (1985) 1171.
22. M. F. LAPPERT, in "Developments in Inorganic Polymer Chemistry", edited by M. F. Lappert and G. J. Leigh (Elsevier, New York, 1962) p. 20.
23. G. CONSTANT and R. FEURER, *J Less-Common Metals* **82** (1981) 113.
24. C. LAFFON, A. M. FLANK, P. LAGARDE, M. LARIDJANI, R. HAGEGE, P. OLRY, J. COTTERET, J. DIXMIER, J. L. MIQUEL, H. HOMMEL and A. P. LEGRAND, *J. Mater. Sci.* **24** (1989) 1503.
25. F. CHRISTIN, R. NASLAIN and C. BERNARD, in "Proceedings of the 7th International Conference on CVD, Los Angeles, edited by T. O. Sedwick and H. Lytdin (The Electrochemical Society, Princeton, NJ, 1979) p. 499.
26. R. NASLAIN, J. Y. ROSSIGNOL, P. HAGENMULLER, F. CHRISTIN, L. HERAUD and J. J. CHOURY, *Rev. Chim. Min.* **18** (1981) 544.
27. R. NASLAIN, F. LANGLAIS and R. FEDOU, *J. de Phys. Coll.* **C5**, suppl. 5,50 (1989) C5-191.
28. S. PROUHET, private communication (1988).
29. E. BOUILLON, D. MOCAER, J. F. VILLENEUVE, R. PAILLER, R. NASLAIN, M. MONTHIOUX, A. OBERLIN, C. GUIMON and G. PFISTER-GUILLOUZO, *J. Mater. Sci.*, submitted.
30. O. DUGNE, S. PROUHET, A. GUETTE, R. NASLAIN, R. FOURMEAUX, K. HSSEIN, J. SEVELY, C. GUIMON, D. GONBEAU and G. PFISTER-GUILLOUZO, *J. de Phys. Coll.* **C5** suppl. 5,50 (1989) C5-333.
31. R. HEZEL and N. LIESKE, *J. Appl. Phys.* **51** (1980) 2566.
32. E. BOUILLON, F. LANGLAIS, R. PAILLER, R. NASLAIN, J. C. SARTHOU, A. DELPUECH, C. LAFFON, P. LAGARDE, F. CRUEGE, P. V. HUONG, M. MONTHIOUX and A. OBERLIN, *J. Mater. Sci.*, submitted.
33. P. MORGEN, K. L. SEAWARD and T. W. BARBEE, *J. Vac. Sci. Technol.* **A3** (1985) 2108.
34. O. DUGNE, S. PROUHET, A. GUETTE, R. NASLAIN and C. BERNARD, *J.* of Alloys and Compounds, **176** (1991) 187.
35. S. SCHAMM, private communication (1989).
36. O. DUGNE and C. BERNARD, private communication (1989).
37. N. T. ZALUZEC, in "Analytical Electron Microscopy", edited by R. H. Geiss (San Francisco Press, 1981) 193.
38. *Idem, Ultramicroscopy* **9** (1982) 319.
39. L. FILIPUZZI, private communication (1989).
40. T. MATSUDA, H. NAKAE and T. HIRAI, *J. Mater. Sci.* **23** (1988) 509.
41. T. MATSUDA, *ibid.* **24** (1989) 2353.
42. A. MARCHAND, G. LACRAMBE and M. TRINQUECOSTE, in "Proceedings of Carbon, 88" Newcastle upon Tyne, edited by B. MacNaney and T. J. Mays (I.O.P. Bristol 1988) p. 355.
43. R. NASLAIN and F. LANGLAIS, in "Tailoring Multiphase and Composite Ceramics", edited by R. E. Tressler, G. L. Messing, G. C. Pantano and R. E. Newnham, Material Science Research, Vol. 20 (Plenum Press, New York, 1986) p. 145.
44. C. J. MACEY, R. L. LEHMAN and R. L. MOORE, *Scanning Electron Microscopy* **IV** (1984) 164.
45. L. PORTE and A. SARTRE, *J. Mater Sci.* **24** (1989) 271.
46. H. ICHIKAWA, T. T. TERANISHI and T. J. ISHIKAWA, *J. Mater. Sci. Lett.* **7** (1987) 420.
47. G. PIGNATEL and G. QUEIROLO, *J. Electrochem. Soc.* **126** (1979) 1805.
48. K. SHOHNO, T. KIM and C. KIM, *ibid.* **127** (1980) 1546.
49. T. MAH, N. L. HETCH, D. E. MACMULLUM, J. R. HOENIGMAN, H. M. KIM. A. P. KATZ and H. A. LIPSITT, *J. Mater. Sci.* **19** (1984) 1191.
50. T. J. CLARK, R. M. ARONS, J. B. STANATOFF and J. RABE, *Ceram. Engng Sci. Proc.* **6** (1985) 576.
51. S. M. JOHNSON, R. D. BRITTAIN, R. H. LAMOREAUX and D. J. ROWCLIFFE, *J. Amer. Ceram. Soc.* **71** (1988) C132.

52. E. MENESSIER, A. GUETTE, R. PAILLER and R. NASLAIN, *C.R. Acad. Sci. Paris*, submitted.
53. E. MENESSIER, A. GUETTE, R. PAILLER and R. NASLAIN, *Compos. Sci. Technol.*, submitted.
54. K. W. PREWO, J. J. BRENNAN and G. K. LAYDEN, *Amer. Ceram. Soc. Bull.* **65** (1986) 305.
55. J. J. BRENNAN, in "Tailoring Multiphase and Composite Ceramics", edited by R. E. Tressler, G. L. Messing, G. C. Pantano and R. E. Newnham, Materials Science Research, Vol. 20 (Plenum Press, New York, 1986) p. 549.
56. R. CHAIM and A. H. HEUER, *Adv. Ceram. Mater.* **2** (1987) 154.
57. E. MENESSIER, Thesis, University of Bordeaux 1 (1988).
58. W. SINCLAIR and H. SIMMONS, *J. Mater. Sci. Lett.* **6** (1987) 627.
59. A. J. CAPUTO, R. A. LOWDEN and D. P. STINTON, ONRL/TM-9651, Available from NTIS, US Department of Commerce, Springfield, VA, June 1985.
60. D. P. STINTON, A. J. CAPUTO and R. A. LOWDEN, *Amer. Ceram. Soc. Bull.* **65** (1986) 347.

Received 19 April 1990
and accepted 15 January 1991